

R.YA. STETSIV, I.V. STASYUK, O. VOROBYOV

Institute for Condensed Matter Physics, Nat. Acad. of Sci. of Ukraine
(1, Svientsitskyi Str., Lviv 79011, Ukraine; e-mail: stetsiv@icmp.lviv.ua)PACS 75.10.Pq, 03.75.Lm,
66.30.Dn**ENERGY SPECTRUM AND STATE DIAGRAMS
OF ONE-DIMENSIONAL IONIC CONDUCTOR**

The energy spectrum for a finite one-dimensional ionic conductor with periodic boundary conditions has been calculated using the exact diagonalization technique. The ionic conductor is described in the framework of the lattice model, with particles obeying the “mixed” Pauli statistics. The model involves the ion transfer, interaction between neighbor ions, and modulating field. One-particle spectral densities are calculated, and phase diagrams are plotted for various temperatures, magnitudes of interaction between particles, and modulating field strengths. Conditions for the transition from the charge-density-wave phase to the superfluid one with the Bose–Einstein condensate (it can be an analog of the superionic phase) and to Mott-insulator type phase are investigated.

Keywords: ionic conductor, spectral density, hard-core boson model, phase diagrams.

1. Introduction

Ionic conductors comprise a wide class of physical and biological objects, and a high interest in them is associated with the possibilities of their practical application. Superionic conductors, which contain a high-temperature phase characterized by a high conductivity, are one of the most interesting examples of those objects. In the low-temperature phase, ions occupy fixed positions. However, after the transition into the superionic phase, they become distributed chaotically with that or another probability over several positions in the elementary cell. A typical example of the superionic crystal can be α -AgJ, where the superionic subsystem is formed by silver ions [1]. In superproton hydrogen-bonded conductors, protons play the role of charge carriers, and they are redistributed over the network of virtual hydrogen bonds [2].

The theoretical description of systems with ionic conductivity is mainly based on lattice models. Some of them consider ions as Fermi particles and focus attention on such issues as the role of long-range interactions [3–5] or the influence of a particle coupling with phonons [6, 7]. In a number of recent works, the attention was paid to short-range interactions between particles [8–10]. However, it should be noted that ions and protons can be described more correctly with the use of the “mixed” Pauli statistics [11], in which, on the one hand, particles are of the bosonic nature and, on the other hand, they are subjected

to Fermi prohibition rules. In comparison with the fermionic approach, this description generates additional complications associated with special commutation rules for the Pauli operators. At the same time, this approach can be more efficient. For instance, it was demonstrated that the Pauli lattice model enables the emergence of a superfluid(SF)-type state, i.e. a phase with the Bose condensate, which can be described even in the absence of a direct interaction between particles [12–14]. To solve the problems of this kind, the Hamiltonian written down in terms of Pauli operators is often reduced with the help of the fermionization procedure [15] (see also works [16–18]) to a Hamiltonian expressed in terms of Fermi operators (only for one-dimensional systems).

The lattice model of Pauli particles is similar to the Bose–Hubbard model in the hard-core boson approximation (provided that the occupation numbers are restricted; $n_i = 0, 1$). This approximation attracts the attention of researchers due to a wide scope of issues, where this model can be applied, proceeding from the theory of quantum-mechanical effects in liquid helium [19, 20]. The model was used to describe the superconductivity of locally coupled electron pairs [14], physical properties of Josephson junctions [21], and ionic conductivity in crystals [11, 12]. The Bose–Hubbard model also describes a transition from the Mott insulator (MI) state into a state of the superfluid (SF) type [22–28]. For the last years, this approach renewed its popularity owing to the researches dealing with the behavior of ultra-cold atoms in op-

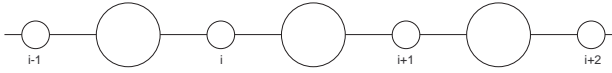


Fig. 1. Model of one-dimensional ionic conductor. Large and small circles denote heavy ionic groups and light mobile ions, respectively

tical lattices. As a rule, the Bose–Hubbard model is used here at arbitrary occupation numbers of local particle positions (see review [29]). The limiting case of this model in the limit of a large on-site repulsion ($U \rightarrow \infty$), when the potential wells are deep enough, is just the hard-core boson model.

In this work, we plot the state diagrams for the ionic conductor, in which particles obey the Pauli statistics. Our lattice model makes includes the ion transfer, interaction between neighbor ions, and modulating field. By applying the exact diagonalization technique, we calculate the one-particle spectral density for finite one-dimensional systems with periodic boundary conditions and, by analyzing the character of those spectra, we obtain the corresponding state diagrams. We also study the conditions required for the transition from the MI phase into the SF-type one (which could be considered as an analog of the superionic phase) to take place, followed by the transition into a state with charge ordering (charge density waves, CDWs).

2. Model of Ionic Conductor

Let us consider the ionic conductor as a chain consisting of heavy motionless ionic groups (large circles in Fig. 1) and light ions, the latter moving along the chain and occupying positions designated by small circles. In such a simplified way, we take into account the Grotthuss mechanism of ion transport in real systems. The subsystem of light ions is described by the Hamiltonian

$$\hat{H} = t \sum_i (c_i^+ c_{i+1} + c_{i+1}^+ c_i) + V \sum_i n_i n_{i+1} - \mu \sum_i n_i + A \sum_i (-1)^i n_i. \quad (1)$$

The model makes allowance for ion motions between neighbor positions (the ion transfer parameter t), the interaction between ions located in neighbor positions (the interaction parameter V), and the modulating field (the parameter A). The field A transforms the system into a two-sublattice one and, to a

certain extent, imitates a long-range interaction between particles, which favors a spatial modulation of the light-ion distribution in the so-called ordered phase (the existence of such a phase at low temperatures is a characteristic feature of superionic conductors). If Hamiltonian (1) is considered in the framework of the Fermi statistics, the corresponding model is known as a spinless fermionic one. This model is widely used in the theory of strongly correlated electron systems [30] and for the description of ionic conductors [31]. A more complicated two-sublattice variant of this model was applied to describe proton conductors [32]. The approach used in this work is based on the “mixed” Pauli statistics. In this case, model (1) is equivalent to the extended hard-core boson model or the boson Hubbard one with repulsive interaction between neighbor particles and strong on-site repulsion ($U \rightarrow \infty$) [33]. The latter is often used while studying the Bose-condensation problems.

3. Exact Diagonalization Technique

In order to calculate the energy spectrum and the spectral densities of a one-dimensional ionic Pauli conductor described by model (1), let us apply the exact diagonalization technique. For this purpose, let us consider a finite chain with periodic boundary conditions. For a chain with N sites in the main region, we introduce the many-particle states

$$|n_1, n_2, \dots, n_N\rangle. \quad (2)$$

In the basis of those states, the Hamiltonian is a $2^N \times 2^N$ matrix and can be diagonalized numerically. This operation corresponds to the transformation

$$U^{-1} H U = \tilde{H} = \sum_p \lambda_p \tilde{X}^{pp}, \quad (3)$$

where λ_p are the Hamiltonian eigenvalues, and \tilde{X}^{pp} are the Hubbard operators. The same transformation is applied to the operators of particle creation and annihilation at the i -th chain site,

$$U^{-1} c_i U = \sum_{pq} A_{pq}^i \tilde{X}^{pq}, \quad U^{-1} c_i^+ U = \sum_{rs} A_{rs}^{i*} \tilde{X}^{rs}, \quad (4)$$

which are used to construct two-time temperature Green’s functions $G_{i,i} = \langle\langle c_i | c_i^+ \rangle\rangle$ containing the information on the one-particle energy spectrum of the

system. For the Pauli creation and annihilation operators, we introduce Green's functions of two types, namely, the commutator Green's function

$$\langle\langle c_i(t)|c_i^+(t')\rangle\rangle^{(c)} = -i\Theta(t-t')\langle[c_i(t), c_i^+(t')]\rangle \quad (5)$$

and the anticommutator one

$$\langle\langle c_i(t)|c_i^+(t')\rangle\rangle^{(a)} = -i\Theta(t-t')\langle\{c_i(t), c_i^+(t')\}\rangle. \quad (6)$$

The imaginary parts of those Green's functions determine one-particle spectral densities,

$$\begin{aligned} \rho(\omega) &= -\frac{1}{\pi N} \sum_{j=1}^N \text{Im} \langle\langle c_j|c_j^+\rangle\rangle_{\omega+i\varepsilon} = \\ &= -\frac{1}{\pi N} \sum_{j=1}^N \text{Im} \left[\frac{1}{Z} \sum_{pq} A_{pq}^j A_{pq}^{j*} \frac{e^{-\beta\lambda_p} - \eta e^{-\beta\lambda_q}}{\omega - (\lambda_q - \lambda_p) + i\varepsilon} \right]. \end{aligned} \quad (7)$$

Here, $Z = \sum_p e^{-\beta\lambda_p}$.

The spectral densities in Eq. (7), which were calculated for the commutator ($\eta = 1$, Eq. (5)) and anticommutator ($\eta = -1$, Eq. (6)) Green's functions, have a discrete structure that includes a number of δ -peaks owing to the finite chain size. If the chain size (the number of sites N) increases, the δ -peaks are located more densely and, at $N \rightarrow \infty$, form a band structure. In our calculations, we confined ourselves to the case $N = 10$. The small parameter Δ was also introduced to broaden the δ -peaks in accordance with the Lorentz distribution

$$\delta(\omega) \rightarrow \frac{1}{\pi} \frac{\Delta}{\omega^2 + \Delta^2}. \quad (8)$$

4. Ion Spectral Densities and State Diagrams

Experimental researches of some specific crystals [34, 35], as well as quantum chemical calculations [36], enable the correlation constant to be evaluated as $V = 3000 \div 10000 \text{ cm}^{-1}$. At the same time, the ion transfer parameter can vary within wide limits, $t = 40 \div 2500 \text{ cm}^{-1}$, depending on the specific objects. Those facts testify that, in real systems, there exists a strong correlation between ions, and this correlation substantially affects the structure and energy spectrum of the system.

We calculated one-particle spectral density (7) in a wide range of magnitudes for the short-range interaction between ions and at various temperatures

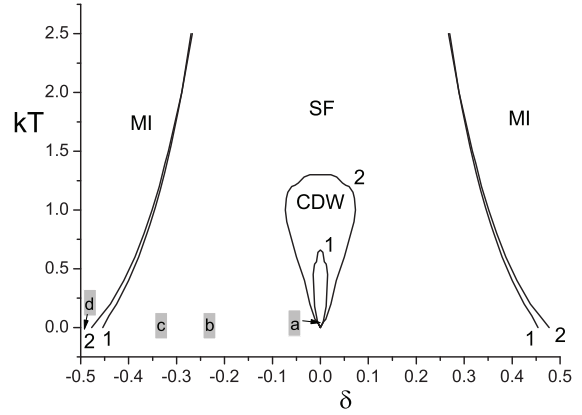


Fig. 2. State diagrams for a one-dimensional ionic conductor at various modulating field magnitudes $A = 0$ (1) and 1 (2). In both cases, $V = 4$, $t = 1$, and $\delta = n - 1/2$

and chemical potentials. In particular, in this work, $V/t = 0, 1, \dots, 6$. All energy parameters, including kT , were normalized by the parameter t , which was, hence, considered as an energy unit. By analyzing the changes in the shape and the character of the calculated frequency dependent spectral densities obtained while varying the model parameters, we plotted the corresponding state diagram (Fig. 2). The average occupation number of the state at a given μ was calculated according to the spectral theorem, $n = \int_{-\infty}^{\infty} \frac{\rho_a(\omega) d\omega}{e^{\beta\omega} + 1}$, where ρ_a is the anticommutator spectral density (the density of states).

When determining the regions of existence for some or other system states (phases), we used the fact that a characteristic feature of the commutator spectral density in the superfluid (SF) phase is the presence of a negative branch ($\omega < 0$), which is a continuous continuation of the positive branch at the point $\omega = 0$ (see, e.g., work [37]). In the case of the phase with charge ordering (CDW), this branch, on the contrary, is separated from the positive one by a gap. Here, the split of the spectrum into two subbands and the emergence of a modulated state with the doubled lattice period are observed.

In the so-called Mott insulator (MI) state, the commutator spectral density has a branch of only one sign. This branch is located at a certain distance from the point $\omega = 0$, which is associated with the location of the chemical potential of particles on the energy scale. The CDW phase is typical of states with the half-filling at $T = 0$. In this case, the chemical poten-

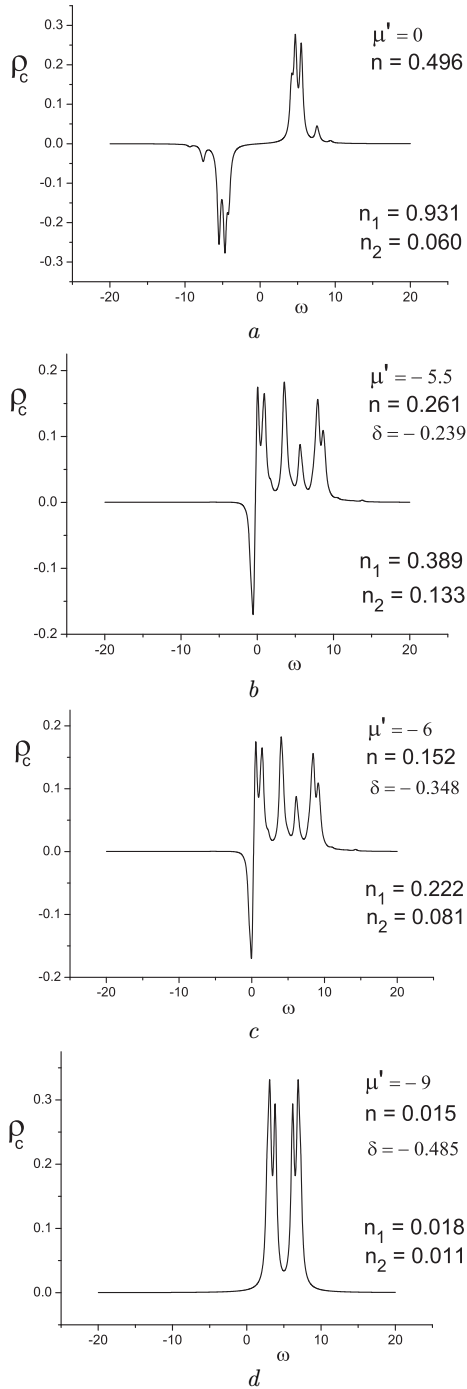


Fig. 3. Commutator one-particle spectral density for various states of a one-dimensional ionic conductor. $T = 0$, $V = 4$, $A = 1$, $t = 1$, and $\Delta = 0.25$. The chemical potential level is located at $\omega = 0$. Panel indices (a to d) coincide with the notation of positions in the diagram in Fig. 2

tial level is located in the energy gap. If the level goes down and moves away from the gap, a transition into the SF phase is observed, with the positive branch continuously transforming into the negative one at $\omega = 0$. If the chemical potential level goes down further, the negative branch disappears, and a transition from the superfluid phase to the phase of the Mott insulator (MI) type takes place, when the chemical potential is located below the lower subband. In this state, a certain activation energy is needed to stimulate the ion transfer. The commutator spectral density has only a positive branch at that. A state of the MI type can also be observed in the case where the chemical potential is located above the upper subband, and the commutator Green's function has only a negative branch.

For the one-dimensional structure under consideration, the CDW, SF, and MI phases described above and the phase transitions between them exist only at zero temperature. At $T \neq 0$, we can distinguish the regions of existence for the states of the CDW, SF, and MI types (see Fig. 2) as such in which the forms of spectral functions characteristic of those phases remain approximately as at $T = 0$. In this case, the transition between the regions is not a true phase transition, but has a crossover character.

Figure 3 exhibits the commutator spectral densities at $T = 0$. The panel indices a to d correspond to the notation of points on the diagram in Fig. 2. The chemical potential position corresponds to the frequency $\omega = 0$. For the sake of convenience, the quantity $\mu' = \mu - V$ was introduced.

Panel a in Fig. 3 is related to the CDW phase, and panels b and c to the SF one, when the negative branch of the commutator spectral density transforms at $\omega = 0$ into the positive one and the gap between them is absent. Panel d corresponds to the MI phase; here, the chemical potential is located below the bottom of the lower subband, and the commutator spectral density has only a positive branch. As one can see from the state diagram (Fig. 2), if $T = 0$, the CDW phase exists only in states with half-filling ($n = 1/2$). In this case, $-4.1 \leq \mu' \leq 4.1$ for the parameter values $V = 4$ and $A = 1$ (at those V - and A -values, the transition CDW-SF occurs at $\mu' = -4.1$ and $+4.1$).

If the temperature grows, the region of existence for the CDW phase becomes smeared, so that it can exist not only at $n = 1/2$, and we obtain

the effect of a temperature-induced transition of the insulator-conductor type (the so-called Mott transition). A possibility for this effect to take place in the objects examined in this work was demonstrated in work [9]. For a similar system described by the Fermi statistics, the existence of this effect was proved with the help of numerical calculations [38]. The mentioned effect can be illustrated with the use of temperature-induced variations in the anticommutator one-particle spectral density (the density of states) (see Fig. 4) calculated on the basis of formula (7). The gap observed in the spectrum ($\rho_a = 0$) at low temperatures and the half-filling is associated with the emergence of a charge-ordered state. The latter originates from the repulsive short-range interaction between particles, which is responsible for the formation of the ground state of this type in the system. At $T \neq 0$, the gap vanishes. On the diagram of states (Fig. 2), the curves correspond to this crossover transition and separate regions, in which the forms of the commutator spectral density ρ_c are closer to those of the function ρ_c for the CDW and SF phases, respectively. The same is also valid for the transitions between the SF and MI phase regions.

An important feature characteristic of the true SF phase is a divergence in the Fourier transform of the real part of commutator Green's function at zero frequency ($\omega = 0$) and zero wave vector ($k = 0$), i.e. $\text{Re } G_{k=0}(\omega = 0) \rightarrow \infty$. In the case of the analyzed finite-chain model,

$$G_{k=0}(\omega = 0) = \frac{1}{N} \sum_{i=1}^N \sum_{j=1}^N \left[\frac{1}{Z} \sum_{pq} A_{pq}^i A_{pq}^{j*} \frac{e^{-\beta\lambda_p} - e^{-\beta\lambda_q}}{\lambda_p - \lambda_q + i\varepsilon} \right]. \quad (9)$$

A numerical calculation shows that the function $\text{Re } G_{k=0}(\omega = 0)$ has finite values in the SF region at $T \neq 0$ (see Fig. 5). This fact confirms that the SF phase is "nongenuine" here; we may call it a phase of the superfluid ("SF") type. The quantity $\text{Re } G_{k=0}(\omega = 0)$, being regarded as a function of the temperature T , diverges only in the limit $T \rightarrow 0$ for some intervals of the chemical potential values, which testifies to an instability of the phase with respect to the appearance of a Bose-condensate in it. However, in the case of a higher space dimension ($d = 2$ or 3), the SF phase can exist at $T \neq 0$ as well.

We calculated the quantity $\text{Re } G_{k=0}(\omega = 0)$ for various values of parameter V describing the interac-

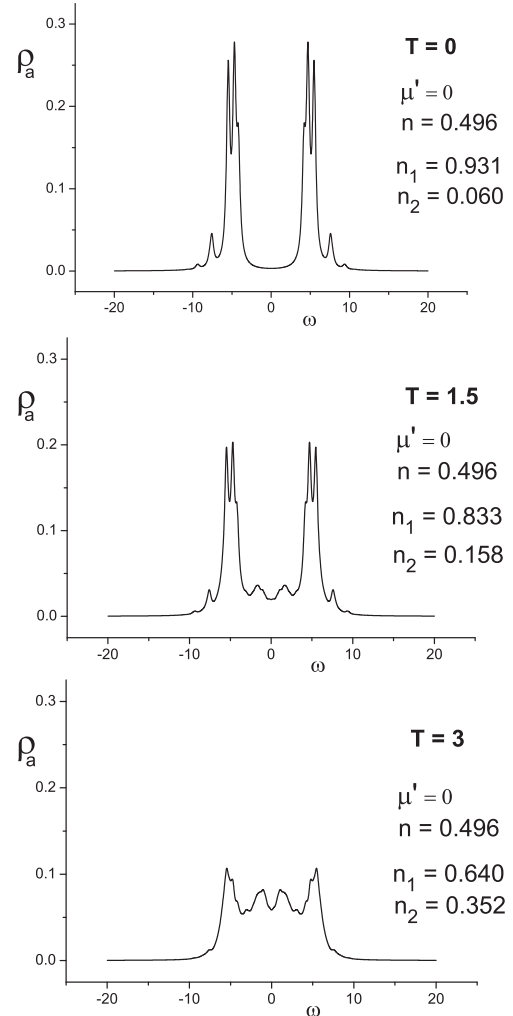


Fig. 4. Closure of the gap in the spectrum of a one-dimensional ionic conductor, as the temperature grows. The case of the half-filling, $n = 1/2$, $\mu' = 0$, $V = 4$, $A = 1$, and $t = 1$. The chemical potential level is located at $\omega = 0$

tion between ions and for various magnitudes of the modulating field A . In all cases, a considerable growth (the maximum) of the function $\text{Re } G_{k=0}(\omega = 0)$ in the "SF" phase region was obtained. However, no peculiarity (the divergence) was observed at $T \neq 0$, and the maximum became smeared out as the temperature increased (see Fig. 5).

Switching-on the modulating field A makes the neighbor positions of ions unequal, and the lattice becomes partitioned in two sublattices with different ionic populations. The modulating field expands the CDW phase region, by simultaneously decreasing the

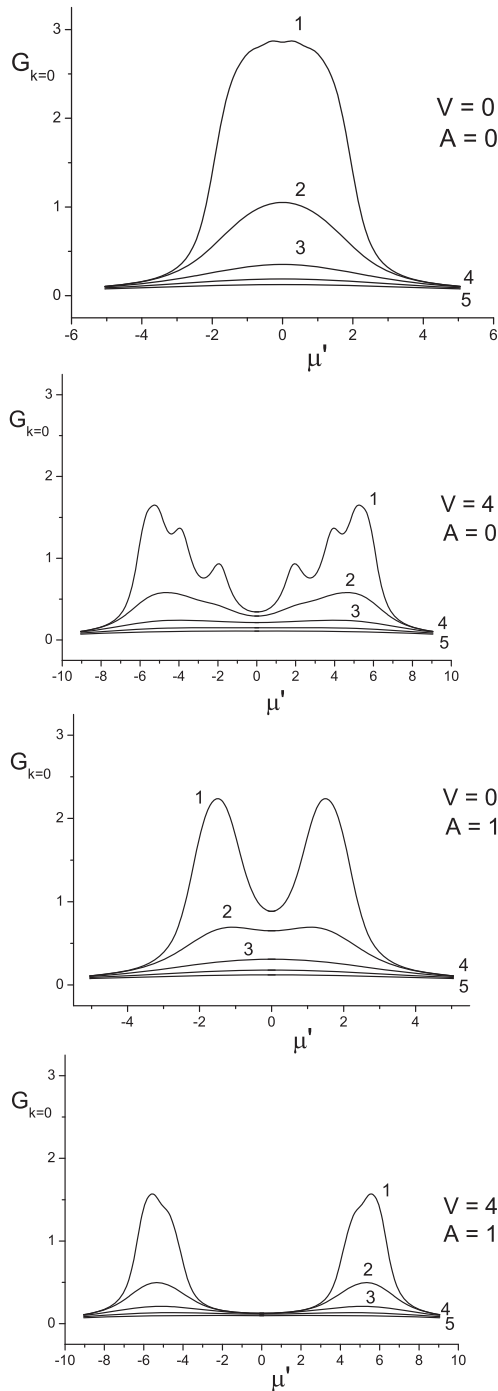


Fig. 5. Fourier transform of the real part of commutator Green's function at zero frequency ($\omega = 0$) and zero wave vector ($k = 0$), $\text{Re } G_{k=0}(\omega = 0)$, for various magnitudes of the interaction between particles, V , and the modulating field, A . $T = 0.2$ (1), 0.5 (2), 1 (3), 1.5 (4), and 2 (5). $\Delta = 1 \times 10^{-6}$

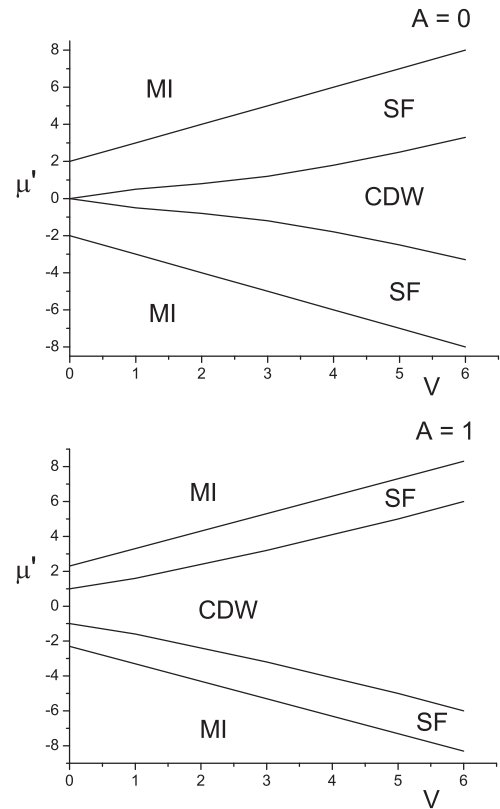


Fig. 6. State diagrams for a one-dimensional ionic conductor in the (μ', V) coordinates in the absence ($A = 0$) and presence ($A = 1$) of a modulating field. $T = 0$

SF one. In work [39], the case $T > 0$ was examined. In this work, the calculations were also carried out for the case $T = 0$. We obtained diagrams that allow one to determine the state of the system at $T = 0$ for a given magnitude of short-range interaction between ions, V , if the modulating field A is either switched-on or -off (Fig. 6). The curve that separates the SF and MI phases was demonstrated to be a straight line, i.e. the value of chemical potential at the transition point is proportional to V .

If either the interaction constant V or the parameter A grows, the gap in the CDW phase spectrum increases. The widening of the gap in the spectrum at growing V was also obtained in previous researches. However, this result was obtained in the case of the Fermi statistics, i.e. in the framework of the spinless fermion model [10, 38]. We also plotted state diagrams for various magnitudes of modulating field A (Fig. 7). In contrast to the previous diagrams,

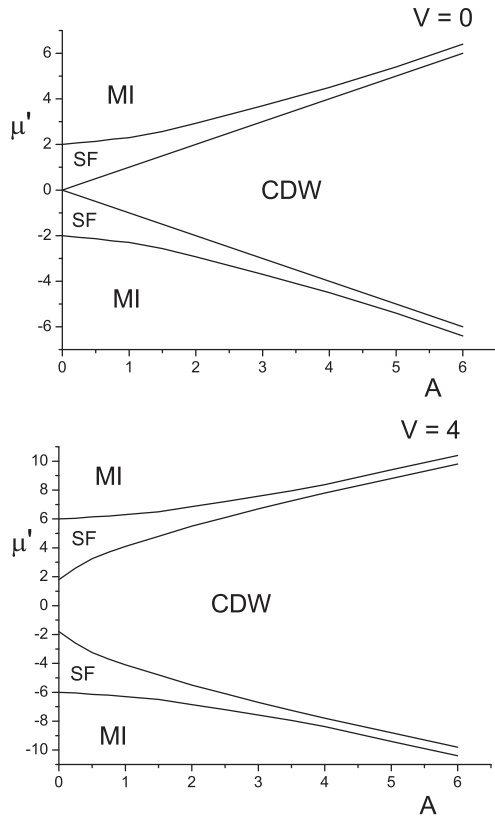


Fig. 7. State diagrams for a one-dimensional ionic conductor in the (μ', A) coordinates in the absence ($V = 0$) and presence ($V = 4$) of interaction between ions. $T = 0$

here, for the case $V = 0$, the straight line separates the CDW and SF phases, whereas the curves that separate the SF and MI phases are characterized by a certain curvature.

The width of the existence region for the CDW phase grows if the magnitude of either the short-range interaction constant V or the modulating field A increases. At $V = 0$, the width of this region is proportional to the modulating field magnitude A (the equations describing the lines separating the CDW and SF phases look like $\mu' = A$ and $\mu' = -A$). In this context, the diagram exhibited in Fig. 7 for the case $V = 0$ coincides with the exact diagram obtained analytically in a number of works dealing with the one-dimensional case (see work [40]). In those works, only the case $V = 0$ was considered, and the diagram was plotted in coordinates different from ours. The exact analytical solution can be obtained in this case, by applying the Jordan–Wigner transformation, which

makes it possible to change from the Hamiltonian of hard-core bosons to the Hamiltonian of noninteracting spinless fermions. Similar researches were carried out in work [12].

5. Conclusions

The results of calculations of the one-particle spectral densities $\rho_c(\omega)$ for a finite one-dimensional ionic conductor carried out in the framework of the hard-core ion model have shown that, depending on the magnitudes of particle chemical potential, short-range interaction constant, and temperature, the form of the function $\rho_c(\omega)$ can change. At $T = 0$, this form corresponds to either the charge-ordered (CDW) or the Mott insulator (MI) phase, or to the so-called superfluid (SF) phase with the Bose condensate. A true CDW phase is realized only at zero temperature and the half-filling of ionic sites ($n = 1/2$). At $T \neq 0$, the interphase boundaries become smeared, and the corresponding phase transitions have a crossover character, i.e. they are not genuine phase transitions. The state diagram in the plane (T, n) is plotted, where the existence regions for the phases of the CDW, MI, and SF types are indicated.

The repulsive short-range interaction between particles ($V > 0$) is shown to result in the emergence of a gap in their energy spectrum at the half-filling of the state. A similar effect also takes place under the influence of the modulating field A , which can be associated with an internal field that appears owing to the long-range interaction (e.g., in the case of a quasi-one-dimensional system composed of chains, the field A can emerge as a result of the interaction between chains). This effect clearly manifests itself at $T = 0$. However, as the temperature grows, the gap becomes gradually filled and, finally, disappears. The increase of the interaction constant V , as well as the field A , makes the gap width wider. At $T = 0$, this circumstance results in that the region of chemical potential values, for which the CDW phase exists, expands.

The Fourier transform of the real part of commutator Green's function of bosons, $\text{Re } G_{k=0}(\omega = 0)$, which is responsible for the static susceptibility of ionic subsystem to the action of the field associated with the creation and annihilation of particles and which describes the system instability with respect to the emergence of a Bose condensate in it, reaches its maximum values in the interval corresponding to the

superfluid (SF) state. At $T = 0$, those values remain finite, which is a result of the restriction imposed on the chain size. On the other hand, as the temperature grows, the maximum of the function $\text{Re } G_{k=0}(\omega = 0)$ becomes smeared, and the tendency to the mentioned instability disappears. This is an additional evidence that the Bose condensate is not formed in the “SF” region in the one-dimensional case and at $T \neq 0$, although the spectral density $\rho_c(\omega)$ is close by its form to the function $\rho_c(\omega)$ for the true SF phase.

1. T. Tomoyose and M. Seino, J. Phys. Soc. Jpn. **67**, 1667 (1998).
2. A.V. Belushkin, V.I.F. David, R.M. Ibberson, and L.A. Shuvalov, Acta Crystallogr. B **47**, 161 (1991).
3. W. Salejda and N.A. Dzhavadov, Phys. Status Solidi B **158**, 119 (1990).
4. W. Salejda and N.A. Dzhavadov, Phys. Status Solidi B **158**, 475 (1990).
5. I.V. Stasyuk, N. Pavlenko, and B. Hilczer, Phase Transit. **62**, 135 (1997).
6. N.I. Pavlenko, Phys. Rev. B **61**, 4988 (2000).
7. V.V. Krasnogolovets and P.M. Tomchuk, Phys. Status Solidi B **130**, 807 (1985).
8. I.V. Stasyuk, O. Vorobyov, and B. Hilczer, Solid State Ionics **145**, 211 (2001).
9. I.V. Stasyuk and O. Vorobyov, Integr. Ferroelectr. **63**, 215 (2004).
10. I.V. Stasyuk and O. Vorobyov, Phase Transit. **80**, 63 (2007).
11. G.D. Mahan, Phys. Rev. B **14**, 780 (1976).
12. I.V. Stasyuk and I.R. Dulepa, Condens. Matter Phys. **10**, 259 (2007).
13. I.V. Stasyuk and I. R. Dulepa, J. Phys. Stud. **13**, 2701 (2009).
14. R. Micnas, J. Ranninger, and S. Robaszkiewicz, Rev. Mod. Phys. **62**, 170 (1990).
15. E. Lieb, T. Schultz, and D. Mattis, Ann. Phys. **16**, 407 (1961).
16. O. Derzhko and T. Krokhnalskii, Phys. Status Solidi B **208**, 221 (1998).
17. O. Derzhko and T. Krokhnalskii, Phys. Status Solidi B **217**, 927 (2000).
18. O. Derzhko, J. Phys. Stud. **5**, 149 (2001).
19. H. Matsuda, and T. Tsuneto, Progr. Theor. Phys. Suppl. **46**, 411 (1970).
20. K. Lin and M. Fisher, J. Low. Temp. Phys. **79**, 251 (1990).
21. G.A. Czathy, J.D. Reppy, and M.H.W. Chan, Phys. Rev. Lett. **91**, 135301 (2003).
22. I.V. Stasyuk and T.S. Mysakovych, Condens. Matter Phys. **12**, 539 (2009).
23. G.G. Batrouni and R.T. Scalettar, Phys. Rev. B **46**, 9051 (1992).
24. R. Micnas and S. Robaszkiewicz, Phys. Rev. B **45**, 9900 (1992).
25. G.G. Batrouni and R.T. Scalettar, Phys. Rev. Lett. **84**, 1599 (2000).
26. K. Bernardet, G.G. Batrouni, J.-L. Meunier, G. Schmid, M. Troyer, and A. Dorneich, Phys. Rev. B **65**, 104519 (2002).
27. K. Bernardet, G.G. Batrouni, and M. Troyer, Phys. Rev. B **66**, 054520 (2002).
28. G. Schmid, S. Todo, M. Troyer, and A. Dorneich, Phys. Rev. Lett. **88**, 167208 (2002).
29. I. Bloch, J. Daliberd, and W. Zwerger, Rev. Mod. Phys. **80**, 885 (2008).
30. R. Vlaming, G.S. Uhrig, and D. Vollhardt, J. Phys.: Condens. Matter **4**, 7773 (1992).
31. B. Lorenz, Phys. Status Solidi B **101**, 297 (1980).
32. I.V. Stasyuk, O.L. Ivankiv, and N.I. Pavlenko, J. Phys. Stud. **1**, 418 (1997).
33. P. Niyaz, R.T. Scalettar, C.Y. Fong, and G.G. Batrouni, Phys. Rev. B **50**, 363 (1994).
34. W. Munch, K.D. Kreuer, U. Traub, and J. Maier, Solid State Ionics **77**, 10 (1995).
35. R. Hassan and E.S. Campbell, J. Chem. Phys. **97**, 4362 (1992).
36. M. Eckert and G. Zundel, J. Phys.Chem. **92**, 7016 (1988).
37. C. Menotti and N. Trivedi, Phys. Rev. B **77**, 235120 (2008).
38. I.V. Stasyuk and O. Vorobyov, Ferroelectrics **376**, 64 (2008).
39. I.V. Stasyuk, O. Vorobyov, and R.Ya. Stetsiv, Ferroelectrics **426**, 6 (2012).
40. I. Hen, M. Iskin, and M. Rigol, Phys. Rev. B **81**, 064503 (2010).

Received 08.10.2013.

Translated from Ukrainian by O.I. Voitenko

Р.Я. Стеців, І.В. Стасюк, О. Воробйов

ЕНЕРГЕТИЧНИЙ СПЕКТР І ДІАГРАМИ СТАНУ ОДНОВИМІРНОГО ІОННОГО ПРОВІДНИКА

Резюме

Методом точної діагоналізації розраховано енергетичний спектр скінченних одновимірних іонних провідників з періодичними граничними умовами. Іонний провідник описується ґратковою моделлю, в якій частинки підлягають “змішаний” статистиці Паулі. У моделі враховується іонне перенесення, взаємодія між сусідніми іонами, а також модулююче поле. Розраховано одночастинкові спектральні густини і отримано діаграми стану для різних температур, різних величин взаємодії і модулюючого поля. Досліджено умови переходу від зарядовпорядкованої фази (CDW) до фази з бозе-конденсатом типу суперфлюїду (SF), яка може бути аналогом суперіонної фази та до фази типу моттівського діелектрика (MI).